Influence of Spatial Variability of Shear Strength Parameters on 3D Slope Reliability and Comparison of Analysis Methods

Varkey, Divya; Hicks, Michael; Vardon, Phil

Publication date
2017

Document Version
Accepted author manuscript

Published in
6th international symposium on geotechnical safety and risk

Citation (APA)
Varkey, D., Hicks, M., & Vardon, P. (2017). Influence of Spatial Variability of Shear Strength Parameters on 3D Slope Reliability and Comparison of Analysis Methods. In *6th international symposium on geotechnical safety and risk: Geo-Risk 2017* (pp. 400-409) http://10.1061/9780784480717.038

Important note
To cite this publication, please use the final published version (if applicable).
Please check the document version above.

Proceedings of the 6th international symposium on geotechnical safety and risk
Geo-Risk 2017, Denver, Colorado | June 4-7, 2017
http://dx.doi.org/10.1061/9780784480717.038

Influence of spatial variability of shear strength parameters on 3D slope reliability and comparison of analysis methods

Divya Varkey,[1] Michael A. Hicks,[2] and Philip J. Vardon[3]

Geo-Engineering Section, Department of Geoscience and Engineering, Delft University of Technology, P.O. Box 5048, 2600 GA Delft, Netherlands; e-mail:
[1]D.Varkey@tudelft.nl [2]M.A.Hicks@tudelft.nl [3]P.J.Vardon@tudelft.nl

ABSTRACT

A 3D slope stability problem with spatially varying shear strength parameters has been analysed using the 3D random finite element method. This method links random fields of the random variables, in this case, cohesion and friction angle, with the finite element method within a Monte Carlo framework. The influence of spatial variability on calculated factors of safety and failure consequence has been investigated, and the results compared with a simpler 3D solution proposed by Vanmarcke. The simpler approach predicted a lower probability of failure under certain conditions, although, at high levels of anisotropy of the heterogeneity, the solutions converged. The reasons for the different solutions have been evaluated.

1. INTRODUCTION

Various attempts have been made to investigate the influence of spatial variability, i.e. heterogeneity, of properties on the factors of safety and reliability of slopes. Of particular interest are slopes which are long in the longitudinal direction, as is often the case for transport embankments and flood defences. A detailed comparison between numerical and analytical approaches was recently made for long slopes characterised by spatially variable undrained shear strength (Li et al., 2015). This involved the random finite element method (RFEM) (Fenton & Griffiths, 2008) and a simpler approach developed by Vanmarcke (1977), based on idealising the failure mechanism as a cylindrical surface with additional resistance at both ends. This was later extended (Vanmarcke, 1980) to general drained and undrained cases, for spatially variable C–ϕ soils governed by the Mohr–Coulomb failure criterion.

Intensive research has reported the influence of spatial variability on the reliability of 2D and 3D soil slopes, as well as on the estimation of spatial correlations, reduction of uncertainty using conditioning, small-probability failure events and combining spatial variability with large deformations; for example, Spencer & Hicks (2007), Griffiths et al. (2009), Arnold & Hicks (2011), Lloret–Cabot et al. (2012), Ji & Chan (2014), Li et al. (2016),

Vardon et al. (2016), de Gast et al. (2017), van den Eijnden et al. (2017) and Wang et al. (2016).

This paper compares the simpler method proposed by Vanmarcke with the more comprehensive, but computationally more intensive, 3D RFEM, where random fields of spatially varying cohesion and friction angle are coupled with the finite element method to compute slope stability within a Monte Carlo framework. A simple slope has been analysed by both methods and the results evaluated.

2. VANMARCKE'S 3D MODEL FOR A GENERAL CASE

Vanmarcke (1977) pioneered analytical 3D slope reliability analysis by assuming a cylindrical failure surface over a finite failure length b along the slope axis, bounded by resisting end sections (see Fig. 1). A 2D cross section at $x=x_0$, was analysed deterministically (Fellenius, 1936), to give the factor of safety:

$$F(x_0) = M_R(x_0)/ M_D(x_0) \tag{1}$$

where $M_R(x_0)$ and $M_D(x_0)$ are the respective resisting and driving moments at $x=x_0$.

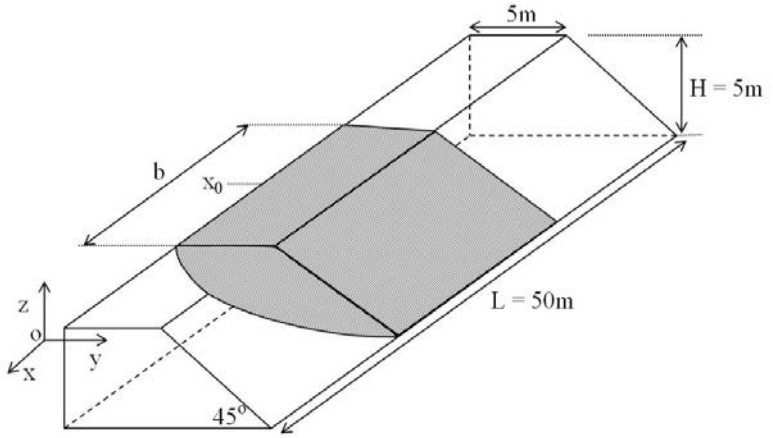

FIG. 1. Problem geometry with cylindrical failure surface

The 3D factor of safety depends on the location of the failure surface, unlike a 2D factor of safety where the failure is independent of slope length. For a failure of length b centred at x_0, the safety factor may be given as:

$$F_b(x_0) = \frac{\text{Resisting moment}}{\text{Driving moment}} = \frac{M_{R,b}(x_0)+R_e}{M_{D,b}(x_0)} \tag{2}$$

$$R_e = M_R d \tag{3}$$

$$\frac{d}{2} = \frac{\text{Sliding area } (A) \text{ of the cross–section}}{\text{Length } (L_a) \text{ of the failure arc}} \tag{4}$$

$$M_{R,b}(x_0) = \int_{x_1}^{x_2} M_R(x)dx \tag{5}$$

where $|x_2 - x_1|$ (=b) is a constant and R_e is the contribution to the resisting moment from the bounding vertical end sections. On moving the centre x_0 along the axis, $M_{R,b}(x_0)$ represents a moving integral of $M_R(x)$.

For a spatially variable shear strength, with spatial correlation governed by the scale of fluctuation (θ), and assuming a deterministic driving moment and neglecting any variance in the end resistance, the mean and standard deviation of the factor of safety, over the failure length b, $\overline{F}_b$ and $\widetilde{F}_b$ respectively, are:

$$\overline{F}_b = \frac{\overline{M}_R b + \overline{R}_e}{\overline{M}_D b} = \overline{F}\,(1 + \frac{d}{b}) \tag{6}$$

$$\widetilde{F}_b = \frac{\widetilde{M}_R b}{\overline{M}_D b} = \overline{F}\, V_s \Gamma(L_a)\Gamma(b) \tag{7}$$

where $\overline{F} = \overline{M}_R / \overline{M}_D$ is the plane strain mean safety factor, V_s is the coefficient of variation of the point shear strength, and $\Gamma(L_a)$ and $\Gamma(b)$ are the reduction factors for shear strength due to averaging, given by:

$$\Gamma(b) = 1; \qquad b \le \theta_h \tag{8a}$$

$$\Gamma(b) = \sqrt{\theta_h / b}; \qquad b > \theta_h \tag{8b}$$

where θ_h is the horizontal scale of fluctuation. $\Gamma(L_a)$ is found by replacing b with the failure arc length L_a and θ_h by the equivalent scale of fluctuation θ_e for an anisotropic case, i.e. when θ is different in the horizontal and vertical directions. The procedure described by Li et al. (2015) is here used to evaluate θ_e.

For the Mohr–Coulomb failure criterion, and assuming no influence of pore pressure, the random shear strength at any point on the failure surface is given as:

$$S = C + NT \tag{9}$$

where, following the notation of Vanmarcke (1980), C is the cohesion, T is the tangent of the friction angle (ϕ) and N is the total normal stress.

Assuming that the random variables may be treated as statistically independent and neglecting any variance in N, the mean and variance of the shear strength at a point may be approximated as:

$$\overline{S} \approx \overline{C} + \overline{N}\,\overline{T} \tag{10a}$$

$$\tilde{S}^2 \approx \tilde{C}^2 + \overline{N}^2 \tilde{T}^2 \quad (10b)$$

The 2D and 3D factors of safety, based on the spatial averages of shear strength along the sliding surface, were given as (Vanmarcke, 1980):

$$\overline{F} = \frac{\overline{M}_R}{\overline{M}_D} = \frac{\overline{S}_1 L_a r}{Wa} \quad (11)$$

$$\overline{F}_b = \overline{F}\,(1 + \frac{d}{b}) \quad (12)$$

$$\tilde{F}_b = \frac{\tilde{S}_b L_a r b}{Wab} = \frac{\tilde{S}_b}{\overline{S}_1}\overline{F} \quad (13)$$

where $\overline{S}_1$ is the averaged shear strength along a unit failure length, $\overline{S}_b$ is the average shear strength along b, L_a is the length of the failure arc, r is the radius, W is the weight per unit failure length of material above the sliding surface and a is the distance between the centre of gravity of the sliding mass and the centre of rotation.

For a stationary random field of shear strength, the average shear strength along the failure length b is $\overline{S}_b = \overline{S}_1 = \overline{S}$. If the standard deviation of cohesion and tangent of friction angle, respectively, along b, are given by $\tilde{C}_b$ and $\tilde{T}_b$, then:

$$\tilde{S}_b = \sqrt{\tilde{C}_b^{\,2} + \overline{N}^2 \tilde{T}_b^{\,2}} \quad (14a)$$

$$\tilde{C}_b = \Gamma(L_a)\Gamma(b)\tilde{C} \quad (14b)$$

$$\tilde{T}_b = \Gamma(L_a)\Gamma(b)\tilde{T} \quad (14c)$$

Both $\overline{F}_b$ and $\tilde{F}_b$ are dependent on b. Assuming a Gaussian distribution for F_b, the probability of failure is given by the area under the curve where $P(F_b \leq 1)$. This probability reaches a maximum for a critical failure length b_c, derived as:

$$b_c = \frac{\overline{F}}{\overline{F} - 1}\, d; \qquad b_c > \theta_h \quad (15a)$$

$$b_c = \theta_h; \qquad b_c \leq \theta_h \quad (15b)$$

3. RANDOM FINITE ELEMENT METHOD (RFEM)

A 3D RFEM model has been used in this paper (e.g. Hicks & Spencer, 2010). Independent random fields for both shear strength variables were generated using local average subdivision (LAS) (Fenton & Vanmarcke, 1990), which requires only the mean, standard

deviation and scales of fluctuation in the three dimensions (θ_x, θ_y and θ_z), where θ_z is the vertical scale of fluctuation (θ_v) and $\theta_x = \theta_y = \theta_h$. Random fields were generated based on the covariance function, β, i.e.,

$$\beta(\tau_x, \tau_y, \tau_z) = \sigma^2 \exp\left(- \frac{2\tau_z}{\theta_z} - \sqrt{\left(\frac{2\tau_x}{\theta_x}\right)^2 + \left(\frac{2\tau_y}{\theta_y}\right)^2} \right) \quad (16)$$

where τ_x, τ_y, τ_z are lag distances in the respective directions and σ is the standard deviation. Here, the authors have generated an isotropic random field using $\theta = \theta_x = \theta_y = \theta_z$ in Eq. (16), and then post-processed this field by squashing and/or stretching in the respective directions to generate the required level of anisotropy, θ_h/θ_v; see Hicks & Samy (2002) and Hicks & Spencer (2010) for details.

Following random field generation, the random field values are mapped to the Gauss points of a finite element mesh. Here, a strength reduction analysis has then been undertaken to determine the factor of safety for each realisation, and multiple realisations performed to determine the distributions of safety factor.

Spencer & Hicks (2007) and Hicks & Spencer (2010) conducted similar 3D RFEM analyses for a cohesive slope with θ_v = 1 m, and proposed three categories of failure mode, for different values of θ_h with respect to the slope height (H) and length (L):

a) *Mode 1* ($\theta_h < H$): Failure propagates through weak and strong zones alike, resulting in considerable averaging of property values along the entire slope length. This is similar to a 2D analysis based on the mean property values.
b) *Mode 2* ($H < \theta_h < L/2$): Failure propagates through semi–continuous weak zones, causing discrete 3D failures and a wide range of possible solutions.
c) *Mode 3* ($\theta_h > L/2$): Failure propagates through weak zones and there is a wider range of possible solutions. The failure impacts the entire slope length, and the solution is analogous to that for a 2D stochastic analysis.

4. PROBLEM DESCRIPTION AND SOLUTIONS

A 3D slope reliability analysis has been carried out on a slope with the dimensions shown in Fig. 1. The finite element mesh uses 20-node hexahedral elements of size 1 m × 1 m × 0.5 m and each element uses 2 × 2 × 2 Gaussian integration. The mesh is fixed at the base, whereas rollers are applied on the back (x–z) face preventing displacements perpendicular to that face, and also on the two end (y–z) faces allowing only vertical displacements (see Hicks & Spencer (2010) for an explanation of these boundary conditions). The soil has a unit weight of 20 kN/m^3, Poisson's ratio of 0.3 and Young's modulus of 1x10^5 kPa. The cohesion and friction angle were considered to be spatially varying and represented by truncated normal distributions, a coefficient of variation of 0.2, and means of 10 kPa and 25^o, respectively. The

same scales of fluctuation are assumed for both parameters; specifically, θ_v = 1 m and a range of values of θ_h.

4.1 Vanmarcke solution (VM)

Based on the given mean values, the plane strain safety factor ($\overline{F}$) was found (using the strength reduction method) to be 1.4, for a 12 m^2 block of soil sliding along a circular arc of length 9.3 m. This failure geometry was determined using finite elements and the same ridge finding procedure reported in Hicks et al. (2014). Based on Eq. (4), d is then computed as 2.58 m.

The procedure to compute the standard deviation of the shear strength along the failure arc was as follows. If C_f and ϕ_f are the reduced values of cohesion and friction angle, respectively, at the onset of failure (see Fig. 2), the average shear and normal stresses at failure along the failure arc are given by:

$$\overline{\sigma}_S \approx (\sum_{i=1}^{N_e} \sigma_s)/N_e \tag{17a}$$

$$\overline{\sigma}_N \approx (\sum_{i=1}^{N_e} \sigma_N)/N_e \tag{17b}$$

where σ_S and σ_N are the shear and normal stresses, respectively, and N_e is the number of elements along the arc. Hence, for a given $\overline{F}$, $\overline{S}_1$ is given as a function of the average shear strength at failure:

$$\overline{S}_1 = \overline{F} \times \overline{\sigma}_s \tag{18}$$

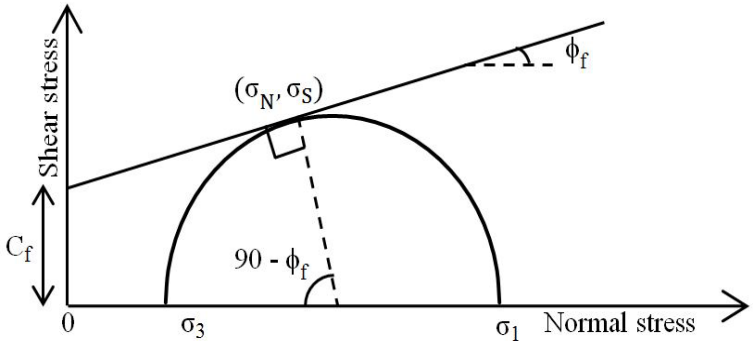

FIG. 2. Stresses at failure

Based on Eqs. (17)–(18) and the assumption of stationary fields, $\overline{S}$ is computed as 17.7 kPa. Considering, as an example, θ_h = 2 m, the critical failure length is calculated using Eq. (15) to be 9.03 m. Since a cylindrical failure mechanism is assumed, this gives a failure volume of 108.4 m^3, which is 5.78% of the total slope volume. Substituting these values into Eq. (12), the mean factor of safety against 3D failure is calculated to be 1.8. The equivalent scale of fluctuation θ_e was determined based on a 1D exponential correlation function, fitted

to the back–figured values along the failure arc (Li et al., 2015). For θ_h = 2 m, $\theta_e \approx$ 1.48 m. Hence, based on the calculated values, the reduction factors are calculated from Eq. (8) as 0.4 and 0.47, due to averaging along the failure arc and failure length, respectively. On substitution into Eq. (14), this gives $\widetilde{C}_b$ = 0.376 kPa, $\tilde{T}_b$ = 0.016 and $\tilde{S}_b$ = 0.46 kPa. Finally, the standard deviation of the factor of safety is estimated as 0.036 using Eq. (13).

Table 1 shows the VM results obtained for all the values of θ_h considered. Note that, for $\theta_h \geq$ 50 m, the critical failure length was limited to the slope length, i.e. 50 m, in calculating the factor of safety statistics.

4.2 RFEM solution

In this section, RFEM results are compared with the VM results for a range of θ_h. A total of 500 Monte Carlo realisations have been performed for each case, which was sufficient to achieve convergence in the mean and standard deviation of the calculated factor of safety. Table 1 compares RFEM and VM solutions for all θ_h.

TABLE 1. Comparison of mean and SD of factors of safety for different θ_h

	θ_h = 1m		θ_h = 2m		θ_h = 6m		θ_h = 12m		θ_h = 24m	
	VM	RFEM	VM	RFEM	VM	RFEM	VM	RFEM	VM	RFEM
Mean	1.8	1.396	1.8	1.382	1.8	1.356	1.71	1.34	1.55	1.34
SD	0.02	0.0108	0.036	0.022	0.07	0.047	0.1	0.059	0.103	0.07

	θ_h = 50m		θ_h = 100m		θ_h = 1000m		θ_h = 2000m		θ_h = 10000m	
	VM	RFEM	VM	RFEM	VM	RFEM	VM	RFEM	VM	RFEM
Mean	1.47	1.348	1.44	1.349	1.41	1.354	1.4	1.39	1.4	1.398
SD	0.105	0.079	0.106	0.085	0.107	0.097	0.107	0.101	0.107	0.104

The mean and standard deviation of F_b depend largely on the predicted failure length. For each realisation, the slide volume is computed on the basis of the elements having an out-of-face displacement more than some calibrated threshold value, as described in Hicks et al. (2008; 2014). For this investigation, this was 37% of the maximum computed out-of-face displacement. The integrated failure length has been calculated as the number of elements in the row, directly above the slope toe, whose out-of-face displacements are greater than the threshold. In Fig. 3, the mean failure volume (as a percentage of the total mesh volume) and failure length from the RFEM analyses, are obtained by averaging over all the realisations for each θ_h.

Figs. 4 (a)–(c) show how the RFEM and VM safety factor distributions (fitted normal) evolve with increasing θ_h. Also plotted are the RFEM slide volumes, from each realisation, against their corresponding factors of safety.

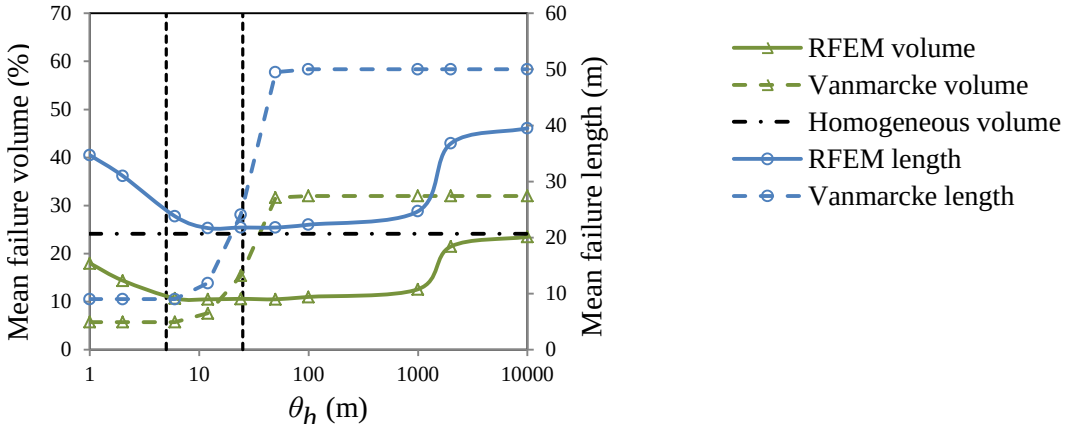

FIG. 3. Comparison of mean failure volume and mean failure length from RFEM analyses with analytical solutions

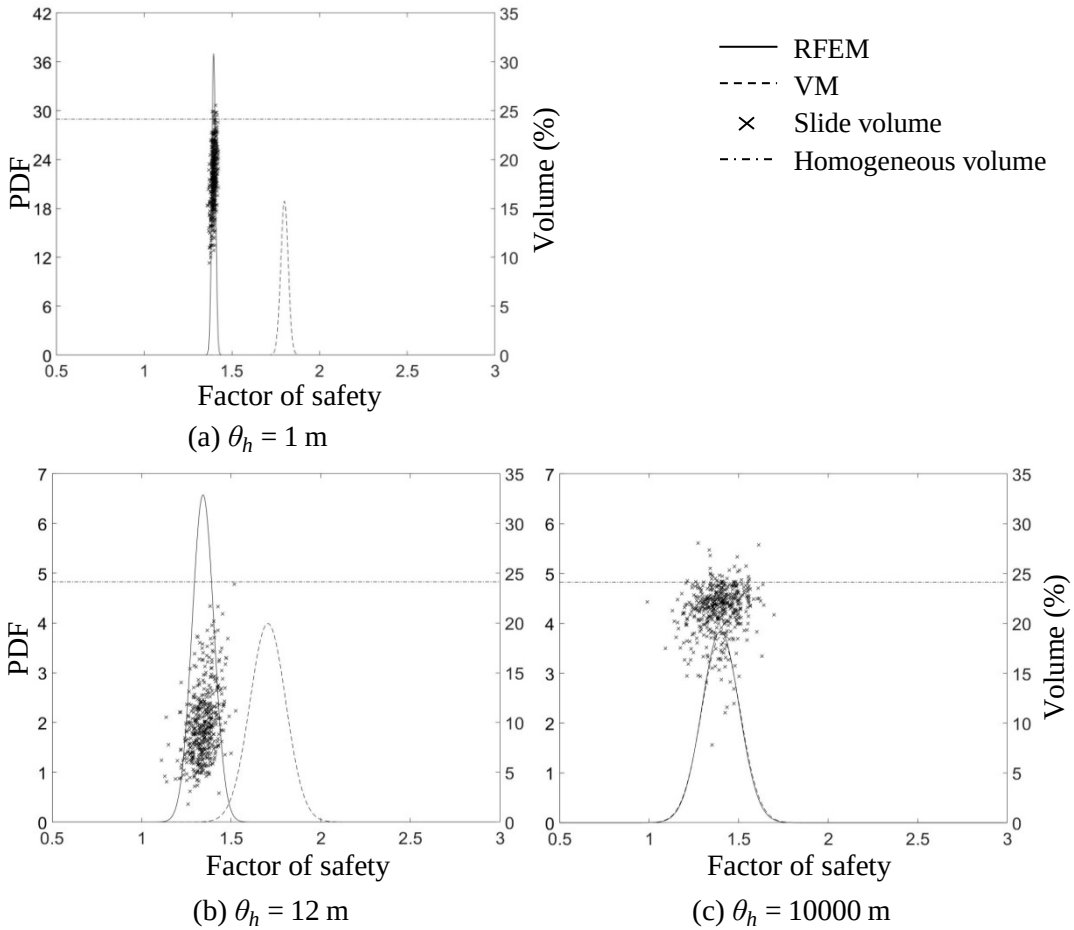

(a) θ_h = 1 m

(b) θ_h = 12 m

(c) θ_h = 10000 m

FIG. 4. PDFs of factor of safety and RFEM failure volumes

The large difference between the two solutions at low θ_h/θ_v is partly due to the considerable averaging of properties and, thereby, to a long failure length and a reduced standard deviation of the factor of safety in the RFEM analysis; and partly due to the short

predicted failure lengths and resulting relatively large contributions from the end resistance in the analytical solution. However, at high levels of θ_h/θ_v, both methods converge to the same 2D solution. The RFEM solutions are consistent with the 3 categories of failure mode described in Section 3. As is seen in Figs. 3–4, convergence to a 2D solution at high θ_h/θ_v is difficult with two random variables. Also, the failure length is shorter than the slope length for failure Modes 1 and 3. This is attributed to the failed zone not reaching the ends of the slope mesh, resulting in shorter (Mode 1 type) failures, due to the boundary conditions which have a greater influence due to the non-zero friction angle.

5. CONCLUSIONS

An idealised 3D slope has been analysed by the random finite element method (RFEM) and a simpler approach developed by Vanmarcke (1980). The relative performance of the two approaches has been investigated by comparing the distributions of factors of safety and failure consequence, quantified in terms of mean failure length and mean slide volume.

The RFEM results confirm three categories of failure mode, which are influenced by the scales of fluctuation relative to the slope dimensions, as found in previous research for an undrained cohesive slope (Hicks & Spencer, 2010; Hicks et al., 2014). For values of θ_h associated with Mode 1 failure using RFEM, the simpler model predicts a larger mean and standard deviation of the factor of safety, due to the shorter predicted failure length. This difference arises because the simpler solution is based on the spatial averages of the shear strength along a predefined cylindrical failure surface, whereas RFEM solutions seek out the weakest failure path along the slope length, resulting in considerable averaging of properties and hence, a reduced standard deviation for a small θ_h/θ_v. Similar findings were reported by Li et al. (2015) for a purely cohesive slope. Conversely, for very large values of θ_h/θ_v, the two methods give similar solutions.

ACKNOWLEDGEMENT

This research is supported by the Dutch Technology Foundation STW, which is part of the Netherlands Organisation for Scientific Research (NWO), and which is partly funded by the Ministry of Economic Affairs.

REFERENCES

Arnold, P. and Hicks, M. A. (2011). “A stochastic approach to rainfall-induced slope failure.” *Proc. 3rd Int. Symp. on Geotech. Safety and Risk*, Munich, Germany, 107–115.

de Gast, T., Vardon, P. J., and Hicks, M. A. (2017). “Estimating spatial correlations under man-made structures on soft soils.” (Accepted) *Proc. 6th Int. Symp. on Geotech. Safety and Risk*, Colorado, USA.

Fellenius, W. (1936). “Calculation of the stability of earth dams.” *Trans. 2nd Congr. on Large Dams*, Washington, USA, 4, 445–459.

Fenton, G. A. and Vanmarcke, E. H. (1990). “Simulation of random fields via local average subdivision.” *J. Eng. Mech.,* ASCE, 116(8), 1733–1749.

Fenton, G. A. and Griffiths, D. V. (2008). *Risk Assessment in Geotechnical Engineering*, John Wiley & Sons, New York.

Griffiths, D. V., Huang, J., and Fenton, G. A. (2009). “On the reliability of earth slopes in 3 dimensions.” *Proc. Royal Soc. A – Math. Phys. Eng. Sciences*, 465(2110), 3145–3164.

Hicks, M. A. and Samy, K. (2002). “Influence of heterogeneity on undrained clay slope stability.” *Quart. J. Eng. Geology and Hydrogeology*, 35(1), 41–49.

Hicks, M. A., Chen, J., and Spencer, W. A. (2008). “Influence of spatial variability on 3D slope failures.” *Proc. 6th Int. Conf. on Computer Simulation in Risk Analysis and Hazard Mitigation,* Cephalonia, Greece, 335–342.

Hicks, M. A. and Spencer, W. A. (2010). “Influence of heterogeneity on the reliability and failure of a long 3D slope.” *Computers and Geotechnics*, 37, 948–955.

Hicks, M. A., Nuttall, J. D., and Chen, J. (2014). “Influence of heterogeneity on 3D slope reliability and failure consequence.” *Computers and Geotechnics,* 61, 198–208.

Ji, J. and Chan, C. L. (2014). “Long embankment failure accounting for longitudinal spatial variation – A probabilistic study.” *Computers and Geotechnics,* 61, 50–56.

Li, Y. J., Hicks, M. A., and Nuttall, J. D. (2015). “Comparative analyses of slope reliability in 3D.” *Eng. Geology,* 196, 12–23.

Li, Y. J., Hicks, M. A., and Vardon, P. J. (2016). “Uncertainty reduction and sampling efficiency in slope designs using 3D conditional random fields.” *Computers and Geotechnics,* 79, 159–172.

Lloret–Cabot, M., Hicks, M. A., and van den Eijnden, A. P. (2012). “Investigation of the reduction in uncertainty due to soil variability when conditioning a random field using kriging.” *Géotechnique Letters*, 2, 123–127.

Spencer, W. A. and Hicks, M. A. (2007). “A 3D finite element study of slope reliability.” *Proc. 10th Int. Symp. on Num. Models in Geomech.,* Rhodes, Greece, 539–543.

van den Eijnden, A. P., Hicks, M. A., and Vardon, P. J. (2017). “Investigating the influence of conditional simulation on small-probability failure events using subset simulation.” (Accepted) *Proc. 6th Int. Symp. on Geotech. Safety and Risk,* Colorado, USA.

Vanmarcke, E. H. (1977). “Reliability of earth slopes.” *J. Geo. Eng*., 103(11), 1247–1265.

Vanmarcke, E. H. (1980). “Probabilistic stability analysis of earth slopes.” *Eng. Geology*, 16, 29–50.

Vardon, P. J., Liu, K., and Hicks, M. A. (2016). “Reduction of slope stability uncertainty based on hydraulic measurement via inverse analysis.” *Georisk: Assess. and Mgmt. of Risk for Eng. Sys. and Geohazards*, 10(3), 1–18.

Wang, B., Hicks, M. A., and Vardon, P. J. (2016). “Slope failure analysis using the random material point method.” *Géotechnique Letters*, 6, 113–118.